analytical chemistry

pubs.acs.org/ac Article

Single-Molecule Biosensing of Alkaline Phosphatase in Cells and Serum Based on Dephosphorylation-Triggered Catalytic Assembly and Disassembly of the Fluorescent DNA Chain

Fei Ma,[†] Ning-ning Zhao,[†] Meng Liu,[†] Qinfeng Xu,* and Chun-yang Zhang*

Cite This: *Anal. Chem.* 2022, 94, 6004−6010 Read Online

ACCESS | Metrics & More | Article Recommendations | Supporting Information

ABSTRACT: Alkaline phosphatase (ALP) is a valuable biomarker and effective therapeutic target for the diagnosis and treatment of diverse human diseases, including bone disorder, cardiovascular disease, and cancers. The reported ALP assays often suffer from laborious procedures, costly reagents, inadequate sensitivity, and large sample consumption. Herein, we report a new single-molecule fluorescent biosensor for the simple and ultrasensitive detection of ALP. In this assay, the ALP-catalyzed dephosphorylation of detection probe can protect the detection probe against lambda exonuclease-mediated digestion, and the remaining detection probes can trigger ceaseless hybridization between two Cy5-labeled hairpin probes through toehold-mediated DNA strand displacement, generating a long fluorescent DNA chain, which can be subsequently separated from unhybridized hairpin probes and disassembled into dispersed Cy5 moieties upon NaOH treatment. The free Cy5 moieties indicate the presence of ALP and can be directly quantified via single-molecule counting. This biosensor enables efficient amplification and transduction of the target ALP signal through enzyme-free assembly and disassembly processes, significantly simplifying the experimental procedure and improving the assay accuracy. The proposed biosensor allows specific and ultrasensitive detection of ALP activity with a detection limit down to 2.61×10^{-6} U mL^{-1} and is suitable for ALP inhibition assay and kinetic analysis. Moreover, this biosensor can be applied for endogenous ALP detection in human cells and clinical human serum, holding the potential in the ALP biological function study and clinical diagnosis.

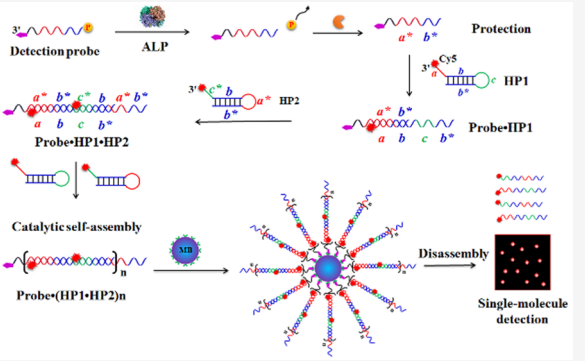

As an essential hydrolytic enzyme that is widely distributed in prokaryotes and eukaryotes, alkaline phosphatase (ALP) acts on phosphorylated substrates to catalyze their dephosphorylation under alkaline conditions through the cleavage of phosphate esters,[1−3] and it partakes in diverse physiological processes including bone mineralization,[4] cell division,[5] immune response,[6] and endotoxin detoxification.[7] An abnormal ALP level is associated with numerous diseases such as bone disorder,[8] primary biliary cirrhosis,[9] stroke,[10] hypophosphatasia,[11] axial spondyloarthritis,[12] diabetes,[13] Wilson's disease,[14] and diverse cancers,[15−18] with great potential as a biomarker for disease diagnosis and prognosis. Bedsides, ALP can serve as a valuable therapeutic target for treatment of various diseases such as cardiovascular disease,[19] inflammatory bowel disease,[20] and vascular calcification.[21] Moreover, ALP is one of the most used enzyme tags in electrochemical assays[22] and is a useful tool enzyme for preventing linear vector religation in the cloning process,[23] end-labeling of nucleic acids,[24] and degrading excess dNTPs in PCR reaction.[25] Therefore, the accurate detection of ALP activity can greatly promote its biological, biomedical, and bioanalysis applications.

A series of ingenious strategies based on fluorescent,[26] chemiluminescent,[27] Raman scattering,[28] colorimetric,[29] electrochemical,[30] and magnetic resonance imaging[31] have been established for sensing ALP activity. Among them, the fluorescent ALP assays are most widely established due to their superiorities of simplicity, stability, rapidity, and sensitivity. However, they often require the complicated synthesis of fluorescent nanomaterials (e.g., quantum dots,[32] gold nanocluster,[33] gold nanocube,[34] copper nanoparticles,[35] graphene quantum dots,[36] silicon nanoparticle,[37] semiconductor quantum dot,[38] and silver nanocluster[39]) or small-molecule fluorescent probes (e.g., near-infrared fluorescent probe,[40] excited-state intramolecular proton transfer florescent probe,[41] two-photon fluorescent probe,[42] excimer/monomer conversion fluorescent probe,[43] and aggregation-induced emission

Received: February 5, 2022
Accepted: March 27, 2022
Published: April 6, 2022

https://doi.org/10.1021/acs.analchem.2c00603
Anal. Chem. 2022, 94, 6004−6010

fluorescent probe[44]). Moreover, non-nucleic acid molecules, including phenolphthalein monophosphate,[45] hydroquinone diphosphate,[46] peptide,[47,48] *p*-nitrophenylphosphate (PNPP),[49] pyrophosphate,[35,39] guanine monophosphate,[50] and adenosine triphosphate,[32] are frequently exploited as the ALP sensing substrates, but they are not easily amplified like DNA/RNA and are not suitable for accurate detection of low-abundant ALP target in rare samples. To overcome this issue, a few nucleic acid signal amplification methods, such as DNA ligase-mediated ligase amplification reaction,[38] DNA polymerase- and nicking enzyme-mediated circular exponential amplification,[51] DNA RNA polymerase- and Cas13a nuclease-mediated RNA transcription-coupled cyclic cleavage reaction,[52] RNA polymerase- and duplex specific nuclease-mediated RNA transcription-induced dual signal amplification,[53] and DNA polymerase- and endonuclease-mediated exponential signal amplification,[54] have been adapted for amplified detection of ALP, but they require multiple specific enzymes to trigger the amplification system, which inevitably increases the assay cost and complicates the reaction process. Besides, the instability of enzyme activities and frequent nonspecific amplification may impair the assay accuracy and reproducibility.

Herein, we constructed a new single-molecule fluorescent biosensor for ALP detection. In this biosensor, the target ALP triggers the assembly of a long fluorescent DNA chain through the enzyme-free hybridization between two fluorescent probes, and the subsequent enzyme-free disassembly of the fluorescent DNA chain produces numerous dispersed fluorescent moieties that can be fluorescently imaged and quantified via single-molecule counting. This biosensor is highly sensitive and it can be employed for endogenous ALP detection in human cells and clinical human serum samples.

EXPERIMENTAL SECTION

Chemicals and Materials. DNA sequences (Table S1) were obtained from Sangon Biotech Co., Ltd. (Shanghai, China). ALP, lambda exonuclease (λ exo), uracil DNA glycosylase (UDG), CpG methyltransfease (MSssI), and streptavidin magnetic beads were purchased from New England Biolabs (Ipswich, MA, U.S.A.). SYBR gold dye was bought from Invitrogen Corporation (California, CA, U.S.A.). The alkaline phosphatase assay kit (pNPP assay) was obtained from beyotime (Haimen, China). The glucoseoxidase (GOX), Na_3VO_4, and bovine serum albumin (BSA) were obtained from Sigma-Aldrich (St. Louis, MO, U.S.A.). Ultrapure water was prepared from a Millipore filtration system (Temecula, CA, U.S.A.).

ALP Detection. To perform ALP-mediated dephosphorylation of detection probes, 10 μL of reaction mixture containing ALP with indicated concentrations, 250 nM detection probe, and 1 μL of 10× CutSmart buffer was reacted at 37 °C for 40 min. Then, 4 U of λ exo was added to react for 30 min at 37 °C. The digestion products were added to 50 μL of solution containing 10 μL of 5× hybridization buffer (50 mM Na_2HPO_4, 0.5 M NaCl, pH 6.8), 400 nM hairpin probe 1 (HP1), and 400 nM hairpin probe 2 (HP2), and the mixture was reacted for 1 h at 37 °C. Then 5 μL of magnetic beads was added to capture the hybridization products, and unreacted H1 and H2 were removed via magnetic separation. After washing the magnetic beads three times with reaction buffer, 50 μL of distilled water containing 1 M NaOH was added to incubate for 5 min to induce the disassembly of the DNA chain, and the supernatant containing free HP1 and HP2 was subjected to measurement.

Ensemble Fluorescence Measurement. The reaction products were measured by fluorescence spectrophotometer (FLS-1000, Edinburgh Instruments, U.K.). The path length of the cuvette was 1 cm, the slit widths for both excitation and emission were set at 4 nm, the excitation wavelength was set at 635 nm, and the emission wavelength of 650−750 nm was measured.

Single-Molecule Counting. For TIRF imaging-based single-molecule counting, the resulting solution was diluted 2000-fold using imaging buffer (1 mg/mL trolox, 50 mM KCl, 5 mM $MgCl_2$, 10 mM Tris-HCl, pH 8.0). The diluted solution was directly dripped on the coverslip and imaged by total internal reflection fluorescence (TIRF) system equipped with a 650 nm laser (50 mW, Coherent, U.S.A.) and a 100× objective (Olympus, Japan). The single-molecule images were obtained by Andor Ixon DU897 EMCCD using 500 ms of exposure time. The 500 × 500 pixels region was used for single-molecule counting. To determine the number of photobleaching steps of the Cy5 spot, the reaction mixture was continuously excited and 50 images were recorded with an exposure time of 400 ms. The data from the images were analyzed using ImageJ software.

Gel Electrophoresis. A total of 20 μL of the reaction products were electrophoresed in 12% nondenaturing polyacrylamide gel using 1× TBE buffer and a voltage of 110 V. After a 1 h electrophoresis, the gel images were obtained by using a gel imaging system (Bio-Rad ChemiDoc MP, CA, U.S.A.).

Detection of ALP Inhibition. The different-concentration ALP inhibitor Na_3VO_4 was preincubated with ALP for 20 min at 37 °C prior to ALP assay. The relative ALP activity (RA) was determined on the basis of eq 1.

$$\mathrm{RA}(\%) = \frac{C_i}{C_t} \times 100\% \tag{1}$$

where C_t and C_i are the ALP activity with and without inhibitor, respectively, and they can be measured based on the linear regression equation $N = 116.38 + 16.34 \log_{10} C$ in Figure 3A. C and N are ALP concentration and Cy5 count number, respectively, and RA can be measured according to eq 2

$$\mathrm{RA}(\%) = \frac{\frac{10^{N_i-23.75}}{21.09}}{\frac{10^{N_t-23.75}}{21.09}} \times 100\% = 10^{N_i-N_t/16.34} \times 100\% \tag{2}$$

where N_i and N_t are the Cy5 count number with and without inhibitor treatment, respectively.

Cell Culture and ALP Extraction. The cell lines, including human cervical cancer HeLa cells, human embryonic kidney HEK cells, and human breast adenocarcinoma MCF-7 cells, were cultured in Dulbecco's modified Eagle's medium containing 1% penicillin−streptomycin and 10% FBS at 37 °C, with the incubator being supplied with 5% CO_2. The cells in the exponential phase of growth were collected and counted using Countstar cell counter (Shanghai, China). The cell extracts were prepared using a nuclear extract kit (ActiveMotif, Carlsbad, CA) and diluted to a certain concentration that is equivalent to an indicated cell number.

https://doi.org/10.1021/acs.analchem.2c00603
Anal. Chem. 2022, 94, 6004−6010

Scheme 1. Dephosphorylation-Triggered the Assembly and Disassembly of Fluorescent DNA Chains for ALP Biosensing[a]

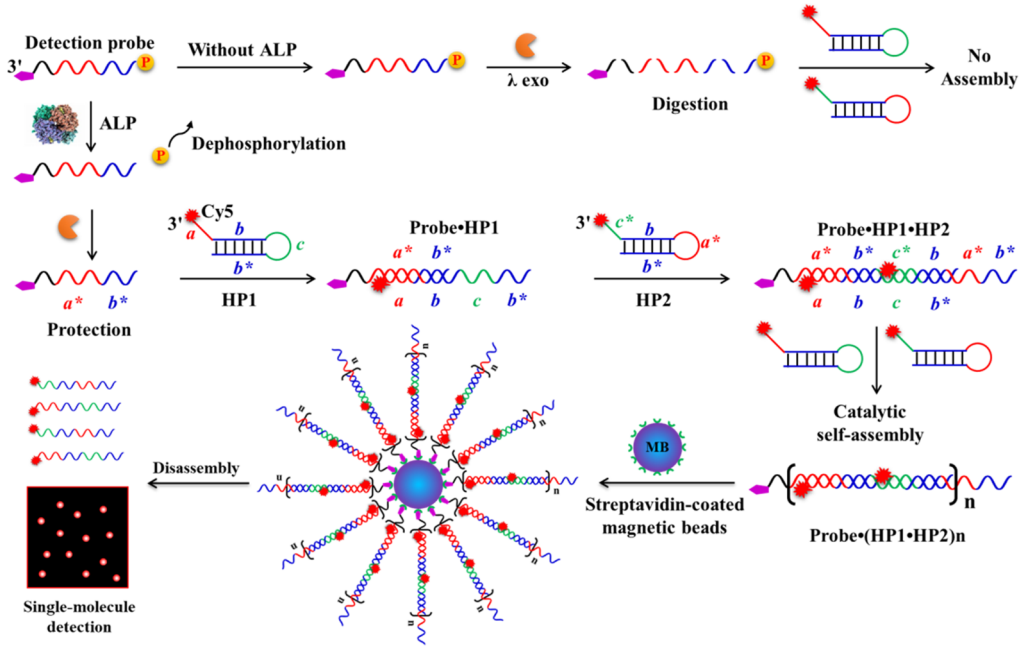

[a]The lowercase letters indicate the functional domains with "*x*" domain being complementary to "*x**" domain.

RESULTS AND DISCUSSION

As shown in Scheme 1, a 5′-phosphorylated ssDNA (Figure S1A) labeled with biotin at the 3′ end is designed as both the detection probe for ALP sensing and the initiator for hybridization chain reaction. When ALP is absent, λ exo can degrade the detection probe from the 5′ to 3′ end,[55] and thus, no hybridization reaction occurs due to the lack of initiator. When ALP is present, ALP dephosphorylates the detection probe through the removal of a phosphate group, which can efficiently protect the detection probe from λ exo digestion.[53] The *a** of the detection probe then binds to a toehold domain *a* of the hairpin probe 1 (HP1, Figure S1B) and triggers the toehold-mediated DNA displacement to form a stable probe·HP1 duplex with the exposure of toehold domain *cb**. Subsequently, the *c** of hairpin probe 2 (HP2, Figure S1C) binds to the *c* of the probe·HP1 duplex and triggers a strand displacement reaction to form a probe·HP1·HP triplex, exposing the toehold domain *b** of HP2, which is identical to the sequence of the probe. Subsequently, the toehold domain *b** of HP2 can bind to new HP1 to trigger the next round of the hybridization reaction. As a result of the ceaseless hybridization between HP1 and HP2, a long fluorescent DNA chain probe·$(HP1{\cdot}HP2)_n$ containing abundant Cy5-labeled HP1 and HP2 are generated, and it can bind to the streptavidin-conjugated magnetic beads via biotin−streptavidin interaction (K_d = 10^{-14} M)[56] and separated from the unhybridized HP1 and HP2 under a magnetic field. After 1 mol/L NaOH treatment,[57] the resulting fluorescent DNA chains are disassembled into free HP1 and HP2, which can be easily imaged by TIRF microscopy and quantified by single-molecule counting. In this biosensor, the magnetic separation enables the isolation of a fluorescent DNA chain from unassembled probes to significantly decrease the background signal, and the subsequent NaOH treatment can disassemble the fluorescent DNA chain into free probes in an enzyme-free manner to facilitate the single-molecule counting of individual signal probe. The integration of these two technologies will allow the simple detection of ALP with high accuracy and sensitivity. In comparison with the reported fluorescent ALP sensors, the proposed biosensor is much simpler by eliminating laborious procedures for the preparation of functional fluorescent nanomaterials[32−39] and small-molecule fluorescent probes,[40−44] and avoiding the enzyme-assisted nucleic acid amplification for ALP signal amplification,[38,51−54] Although it cannot be applied for the imaging of ALP activity in living cells like some reported fluorescent ALP assays,[40,42] the proposed ALP biosensor can sensitively detect ALP in cell extracts and serum samples.

We verified the ALP-mediated protection of detection probe using nondenaturing polyacrylamide gel electrophoresis (12%) and DNA dye SYBR gold (it emits strong green fluorescence signal upon binding with nucleic acids).[58] As shown in Figure 1A, after λ exo treatment, no band is observed when ALP is absent (Figure 1A, lane 1), suggesting the degradation of detection probe in the absence of target. In contrast, a distinct band of detection probe is detected when ALP is present (Figure 1A, lane 2), suggesting the ALP-directed protection of detection probe from λ exo digestion. We further employed PAGE to analyze the ALP-triggered self-assembly reaction through direct excitation of Cy5 molecules (Figure 1B). When ALP is absent, only the bands of HP1 and HP2 are observed (Figure 1B, lane 1), with similar results observed in groups without a detection probe (Figure 1B, lane 2), indicating no occurrence of an assembly reaction due to the complete digestion of detection probes without ALP. In contrast, an obvious dispersion band is generated in the presence of ALP, demonstrating the successful ALP-directed assembly of fluorescent DNA chains of probe·$(HP1{\cdot}HP2)_n$. In fluorescence imaging experiments, a distinct fluorescence signal is produced around the magnetic beads when ALP is present, but it disappears when ALP is absent (control, Figure 1C), indicating the ALP-mediated assembly of fluorescent DNA chains on the magnetic beads. Furthermore, the reaction products are

https://doi.org/10.1021/acs.analchem.2c00603
Anal. Chem. 2022, 94, 6004−6010

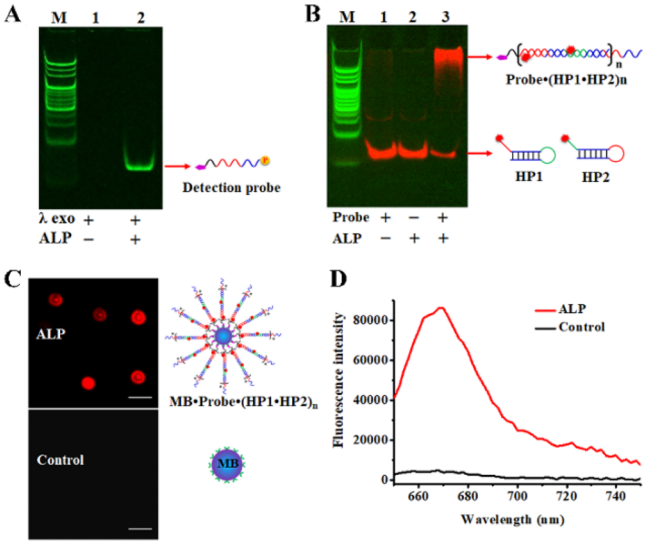

Figure 1. (A) PAGE analysis of ALP-directed protection of detection probe from λ exo digestion. Lane M: 20 bp DNA Ladder; lane 1: λ exo; lane 2: λ exo + ALP. Both DNA marker and reaction products were stained with SYBR gold dye. (B) PAGE analysis of the assembly of fluorescent DNA chains induced by ALP. Lane M: 20 bp DNA Ladder; lane 1: detection probe; lane 2: ALP + detection probe; lane 3: λ exo + ALP. (C) Imaging of magnetic beads without (control, bottom) and with (top) ALP. Scale bar = 10 μM. (D) Fluorescence spectra with (red color) and without (control, black color) ALP. The 4 U of λ exo, 0.1 U/mL ALP, 250 nM detection probe, 400 nM HP1, and 400 nM HP2 were used in B−D.

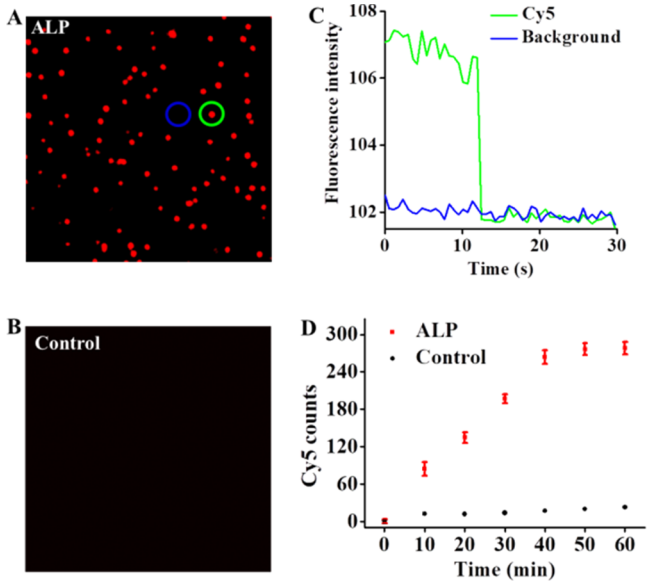

Figure 2. (A) Images of single Cy5 moieties in response to ALP. (B) Images of single Cy5 moieties without ALP (control). A single Cy5 spot and the background are indicated by green and blue circles, respectively. (C) Fluorescence intensity traces of the fluorescent spot (green color) and background (blue color) over time showing a one-step photobleaching. (D) Variance of Cy5 counts as a function of incubation time with (red color) and without (control, black color) ALP. The 0.1 U/mL ALP was used in the experiments.

disassembled from magnetic beads, and the supernatant is subjected to fluorescence measurement (Figure 1D). No obvious fluorescence is generated without ALP (control, Figure 1D, black line), while a strong fluorescence signal with a peak wavelength of 670 nm is produced in response to ALP (Figure 1D, red line), suggesting efficient signal amplification induced by ALP. These results indicate that this biosensor can be applied for the monitoring of ALP activity.

Different from traditional fluorescent assays that measure the ensemble average,[59] single-molecule fluorescence detection can efficiently eliminate the inner filter effect to allow the visualization and quantification of individual target molecules with high resolution and extremely low sample consumption.[60] We employed single-molecule imaging to monitor the ALP-derived Cy5 signal. Distinct Cy5 fluorescent spots are detected at the excitation wavelength of 640 nm upon the addition of 0.1 U/mL ALP (Figure 2A), but no fluorescent spot is detected in the control group without ALP (Figure 2B). Notably, the Cy5 spot demonstrates a one-step photobleaching (Figure 2C), suggesting that each fluorescent spot contains a single Cy5 molecule. The time-course experiment (Figure 2D) indicates that the Cy5 counts are enhanced with incubation time and reach saturation beyond 40 min. In contrast, no significant change is observed in the Cy5 signal in the control group. These results verify the achievement of single-molecule counting of the ALP activity.

We investigated the assay sensitivity by measuring the Cy5 counts produced by different-concentration ALP under optimized reaction conditions (i.e., λ exo amount of 4 U, λ exo incubation time of 30 min, hybridization reaction time of 1 h, Figures S2−S4). The Cy5 counts (N) enhance when the ALP concentration (C) increases from 0 to 2 U mL^{-1} (Figure 3A), and they exhibit a linear correlation with the logarithm of ALP concentration from 1×10^{-5} to 1×10^{-2} U mL^{-1}. The regression equation is $N = 104.36 + 16.29 \log_{10}C$ (R^2 =

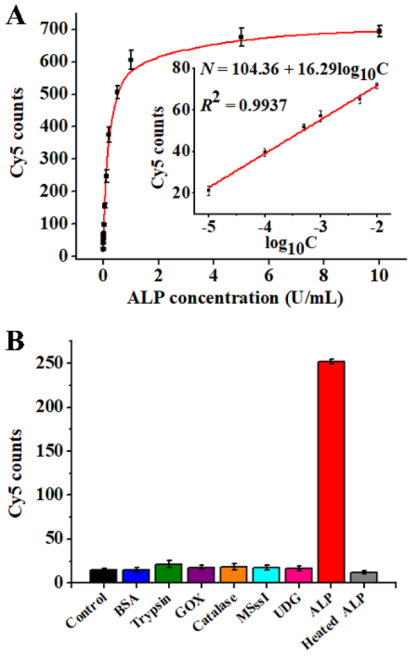

Figure 3. (A) Variance of Cy5 counts as a function of ALP concentration. The inset shows the linear dependence of Cy5 counts upon ALP concentration from 1×10^{-5} to 1×10^{-2} U/mL. (B) Cy5 counts generated by BSA, trypsin, GOX, catalase, MSssI, UDG, ALP, and heated ALP, respectively. The 100 mg/L BSA, 100 mg/L trypsin, 100 mg/L GOX, 100 mg/L catalase, and 0.1 U/mL MSssI, 0.1 U/mL UDG, and 0.1 U/mL ALP were used in the experiments.

https://doi.org/10.1021/acs.analchem.2c00603
Anal. Chem. 2022, 94, 6004−6010

0.9937). The detection limit is calculated to be 2.61× 10^{-6} U mL^{-1} based on $3\sigma/K$ (σ and K are the standard deviation of control sample and the slope of calibration curve), which is superior to the reported ALP assays (Table S2). The high sensitivity can be attributed to the following three factors: (1) the low background signal generated by the complete digestion of excess phosphorylated probes by λ exo and the separation of unhybridized hairpin probes from the assembled DNA chains, (2) efficient target signal amplification and transduction induced by catalytic assembly and disassembly processes, and (3) the inherent high sensitivity of single-molecule detection.

We further investigate the selectivity of this biosensor using various nonspecific enzymes including BSA, GOX, trypsin, catalase, MSssI, and UDG. A significantly amplified Cy5 signal is generated when target ALP is present, and no signal improvement is detected in response to BSA, trypsin, GOX, catalase, MSssI, UDG, and a control group without any enzymes. Notably, the Cy5 signal produced by heated ALP is identical to that of the control group without any enzymes, suggesting the complete loss of ALP activity upon heat treatment. This result indicates the excellent specificity of this biosensor toward ALP.

We further employed this biosensor to analyze ALP enzyme kinetic parameters. The initial ALP reaction velocity (V) in response to different concentrations of detection probe was measured, and the data were fitted to the Michaelis−Menten equation of $V = \frac{V_{max}[S]}{K_m + [S]}$, where V_{max}, $[S]$, and K_m are the maximum initial velocity, detection probe concentration, and Michaelis−Menten constant, respectively. The initial velocity enhances when the detection probe concentration increases from 0 to 250 nM. The K_m and V_{max} are measured to be 260.96 nM and 29.97 min^{-1}, respectively, suggesting that the proposed biosensor is suitable for ALP kinetic analysis.

ALP inhibitors are regarded as promising drugs for the treatment of various diseases, such as vascular smooth muscle cell calcification[61] and cardiovascular disease.[19] We used sodium orthovanadate (Na_3VO_4)[53] as a competitive ALP inhibitor to demonstrate the capability of the proposed biosensor for inhibition assay. The relative ALP activity (RA) exhibits a dose-dependent decrease with Na_3VO_4 concentration from 10 to 400 μM (Figure 4B). The IC_{50} (the concentration of Na_3VO_4 with the capability to reduce 50% ALP activity) is determined to be 78.65 μM, which is in agreement with that obtained by polymer dot-based immunoassay (25.9 μM)[62] and coordination polymer nanoparticle-based fluorescent assay (148.6 μM),[63] suggesting the potential of the proposed biosensor for ALP-targeted drug discovery.

Dysregulated cellular ALP activity is implicated in diverse human diseases including cancers.[15−18] We further verified the feasibility of this biosensor for cellular ALP assay (Figure 5A). The control group without cell extracts only generates a low background signal. In contrast, distinct Cy5 signal is detected in HEK cells, HeLa cells and MCF-7 cells, with the decrease of Cy5 signal in the order of HeLa cells > MCF-7 cells > HEK cells, indicating different cellular ALP activity levels in different cell lines, which is consistent with previous researches,[38,53] suggesting that the proposed biosensor can discriminate ALP level between cancer cells and normal cells and even among different cancer cell lines. Moreover, the Cy5 counts (N) improve when HeLa cell number (X) increases from 0 to 10000 cells (Figure 5B), and they exhibit a linear dependence upon the HeLa cell number from 10 to 10000 cells in a logarithm scale, with the equation being $N = -0.0471 + 21.27 \log_{10} X$. The detection limit is determined to be two cells. Notably, the treatment of HEK, MCF-7, and HeLa cells with Na_3VO_4 induces the decrease of the Cy5 signal, suggesting the efficient inhibition of endogenous ALP activity by Na_3VO_4. These results demonstrate the feasibility of this biosensor for sensitive and accurate detection of endogenous ALP in human cells.

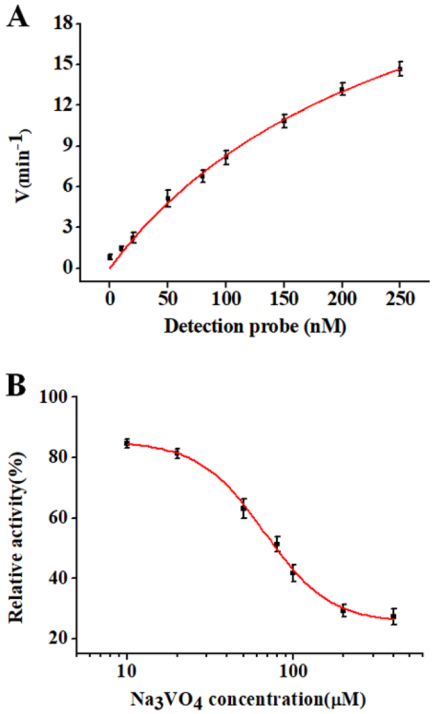

Figure 4. (A) Variance of initial ALP reaction rate as a function of detection probe concentration. (B) Variance of relative ALP activity as a function of Na_3VO_4 concentration.

We further measured ALP in clinical serum samples using the proposed biosensor. The ALP can be quantitatively detected in 10 serum samples with an average concentration of 82.3 U/L (Figure 6A, red column), which is identical to that obtained by standard pNPP assay with an average concentration of 80.8 U/L (Figure 6A, black column). Moreover, ALP can be detected from a series of diluted serum with volumes from 0 to 1 μL, and even ALP from 0.05 μL of serum can be well discriminated from the control samples without serum. The sample consumption of the proposed biosensor (0.05 μL) is 100× lower than that required in p-nitrophenyl phosphate-based colorimetric ALP assay (5 μL),[64] suggesting that the proposed biosensor can detect the serum ALP level with high accuracy and minimum sample consumption.

CONCLUSIONS

We have constructed a new single-molecule fluorescent biosensor for accurate and sensitive monitoring of ALP level in human cells and clinical serum samples. All probes involved in this biosensor are commercially available, which avoids laborious procedures for the preparation of functional fluorescent nanomaterials[32−39] and small-molecule fluorescent probes.[40−44] Superior to enzyme-assisted nucleic acid amplification-based ALP assays,[38,51−54] the signal amplification and transduction involved in this biosensor can be achieved with enzyme-free assembly and disassembly processes, greatly

https://doi.org/10.1021/acs.analchem.2c00603
Anal. Chem. 2022, 94, 6004−6010

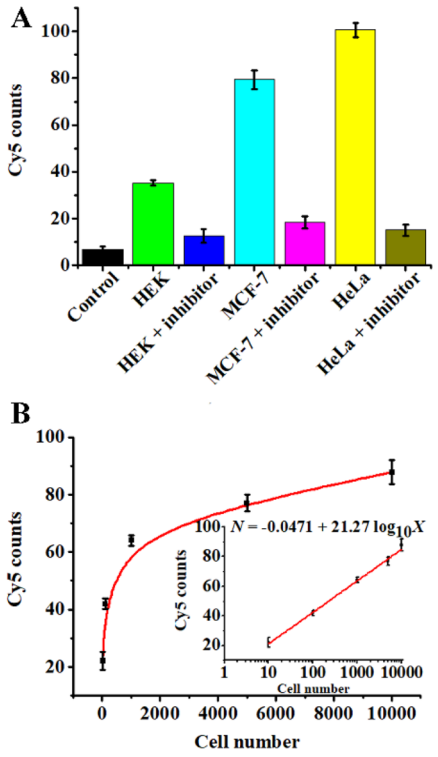

Figure 5. (A) Comparison of Cy5 counts generated by HEK cells (green column), HEK cells + Na_3VO_4 (blue column), MCF-7 cells (cyan column), MCF-7 cells + Na_3VO_4 (pink column), Hela cells (yellow column), Hela cells + Na_3VO_4 (brown column), and the control (black column). The 10000 cells and 200 μM Na_3VO_4 were used in the experiments. (B) Variance of Cy5 counts as a function of HeLa cell number from 0 to 10000 cells. Inset shows the linear dependence of Cy5 counts upon HeLa cell number from 10 to 10000 cells.

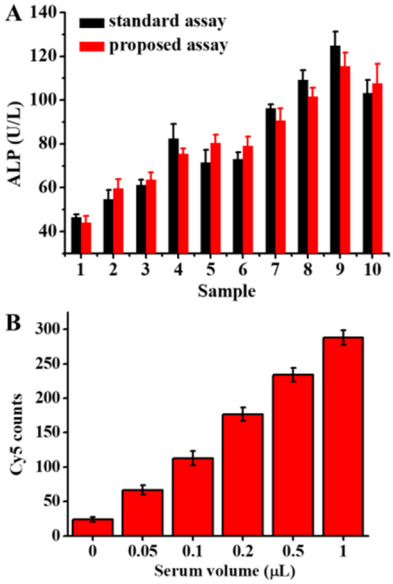

Figure 6. (A) Measurement of ALP level in clinical serum samples using the proposed biosensor (red column) and the standard pNPP assay (black column). (B) Measurement of Cy5 counts in response to serum volume from 0 to 1 μL.

simplifying the assay procedures and eliminating nonspecific signals. This biosensor can sensitively detect ALP activity with a detection limit of 2.61×10^{-6} U/mL, and it can be applied for ALP inhibition assays and kinetic analysis. Importantly, this biosensor can accurately detect the endogenous ALP level in human cells and clinical serum samples with minimum sample consumption, providing a new platform for ALP-related biological research and clinical diagnosis. Furthermore, this biosensor can be extended to detect other nucleic acids and nucleic acid-modifying enzymes by using corresponding probes and recognition enzymes.

■ ASSOCIATED CONTENT

Supporting Information

The Supporting Information is available free of charge at https://pubs.acs.org/doi/10.1021/acs.analchem.2c00603.

Sequences of synthesized oligonucleotides, predicted secondary structure of probes, optimization of the assay conditions, and a comparison of the proposed biosensor with the reported ALP assays (PDF)

■ AUTHOR INFORMATION

Corresponding Authors

Chun-yang Zhang − *College of Chemistry, Chemical Engineering and Materials Science, Shandong Normal University, Jinan 250014, China;* orcid.org/0000-0002-8010-1981; Email: cyzhang@sdnu.edu.cn

Qinfeng Xu − *School of Food and Biological Engineering, Shaanxi University of Science and Technology, Xi'an 710021, China*; Email: xuqinfeng@sust.edu.cn

Authors

Fei Ma − *College of Chemistry, Chemical Engineering and Materials Science, Shandong Normal University, Jinan 250014, China; School of Chemistry and Chemical Engineering, Southeast University, Nanjing 211189, China*

Ning-ning Zhao − *College of Chemistry, Chemical Engineering and Materials Science, Shandong Normal University, Jinan 250014, China*

Meng Liu − *College of Chemistry, Chemical Engineering and Materials Science, Shandong Normal University, Jinan 250014, China*

Complete contact information is available at: https://pubs.acs.org/10.1021/acs.analchem.2c00603

Author Contributions

†These authors contributed equally to this work.

Notes

The authors declare no competing financial interest.

■ ACKNOWLEDGMENTS

This work was supported by the National Natural Science Foundation of China (Grant Nos. 21735003 and 22174017) and the Award for Team Leader Program of Taishan Scholars of Shandong Province, China.

■ REFERENCES

(1) Fishman, W. H.; Inglis, N. I.; Stolbach, L. L.; Krant, M. J. *Cancer Res.* **1968**, *28*, 150−154.

(2) Coleman, J. E. *Annu. Rev. Biophys. Biomol. Struct.* **1992**, *21*, 441−483.

(3) Sharma, U.; Pal, D.; Prasad, R. *Indian J. Clin. Bioche.* **2014**, *29*, 269−278.

(4) Golub, E. E.; Boesze-Battaglia, K. *Curr. Opin. Orthop.* **2007**, *18*, 444−448.
(5) Bhatti, A.; DeVoe, I.; Ingram, J. *J. Bacteriol.* **1976**, *126*, 400−409.
(6) Rader, B. A. *Front. Immunol.* **2017**, *8*, 897.
(7) Poelstra, K.; Bakker, W. W.; Klok, P. A.; Hardonk, M. J.; Meijer, D. *Lab. Invest.* **1997**, *76*, 319−327.
(8) Sardiwal, S.; Magnusson, P.; Goldsmith, D. J. A.; Lamb, E. J. *Am. J. Kidney Dis.* **2013**, *62*, 810−822.
(9) Lammers, W. J.; van Buuren, H. R.; Hirschfield, G. M.; Janssen, H. L. A.; Invernizzi, P.; Mason, A. L.; Ponsioen, C. Y.; Floreani, A.; Corpechot, C.; Mayo, M. J.; Battezzati, P. M.; Parés, A.; Nevens, F.; Burroughs, A. K.; Kowdley, K. V.; Trivedi, P. J.; Kumagi, T.; Cheung, A.; Lleo, A.; Imam, M. H.; et al. *Gastroenterology* **2014**, *147*, 1338−1349.
(10) Brichacek, A. L.; Brown, C. M. *Metab. Brain Dis.* **2019**, *34*, 3−19.
(11) Mornet, E. *Hum. Mutat.* **2000**, *15*, 309−315.
(12) Kang, K. Y.; Hong, Y. S.; Park, S.-H.; Ju, J. H. *Semin. Arthritis Rheum.* **2015**, *45*, 202−207.
(13) Berberoglu, Z.; Gursoy, A.; Bayraktar, N.; Yazici, A. C.; Bascil Tutuncu, N.; Guvener Demirag, N. *J. Clin. Endocr. Metab.* **2007**, *92*, 3523−3530.
(14) Hirani, T. A.; Suzuki, I.; Murata, N.; Hayashi, H.; Eaton-Rye, J. J. *Plant Mol. Biol.* **2001**, *45*, 133−144.
(15) Rao, S. R.; Snaith, A. E.; Marino, D.; Cheng, X.; Lwin, S. T.; Orriss, I. R.; Hamdy, F. C.; Edwards, C. M. *Br. J. Cancer* **2017**, *116*, 227.
(16) Min, J.-W.; Um, S.-W.; Yim, J.-J.; Yoo, C.-G.; Han, S. K.; Shim, Y.-S.; Kim, Y. W. *J. Korean Med. Sci.* **2009**, *24*, 275−280.
(17) Xiao, B.; Guo, J.; Liu, D.; Zhang, S. *Oral Oncol.* **2007**, *43*, 905−910.
(18) Nathanson, L.; Fishman, W. H. *Cancer* **1971**, *27*, 1388−1397.
(19) Haarhaus, M.; Brandenburg, V.; Kalantar-Zadeh, K.; Stenvinkel, P.; Magnusson, P. *Nat. Rev. Nephrol.* **2017**, *13*, 429−442.
(20) de Medina, F. S.; Martínez-Augustin, O.; González, R.; Ballester, I.; Nieto, A.; Gálvez, J.; Zarzuelo, A. *Biochem. Pharmacol.* **2004**, *68*, 2317−2326.
(21) Azpiazu, D.; Gonzalo, S.; Villa-Bellosta, R. *Curr. Cardiol. Rev.* **2019**, *15*, 91−95.
(22) Li, X.-M.; Yang, X.-Y.; Zhang, S.-S. *TrAC-Trend. Anal. Chem.* **2008**, *27*, 543−553.
(23) Aslanidis, C.; De Jong, P. J. *Nucleic Acids Res.* **1990**, *18*, 6069−6074.
(24) Kobori, H.; Sullivan, C. W.; Shizuya, H. *P. Natl. Acad. SCI. U.S.A.* **1984**, *81*, 6691−6695.
(25) Dugan, K. A.; Lawrence, H. S.; Hares, D. R.; Fisher, C. L.; Budowle, B. *J. Forensic Sci.* **2002**, *47*, 15459J.
(26) Qian, Z. S.; Chai, L. J.; Huang, Y. Y.; Tang, C.; Shen, J. J.; Chen, J. R.; Feng, H. *Biosens. Bioelectron.* **2015**, *68*, 675−680.
(27) Bronstein, I.; Voyta, J.; Thorpe, G.; Kricka, L.; Armstrong, G. *Clin. Chem.* **1989**, *35*, 1441−1446.
(28) Ruan, C.; Wang, W.; Gu, B. *Anal. Chem.* **2006**, *78*, 3379−3384.
(29) Li, C. M.; Zhen, S. J.; Wang, J.; Li, Y. F.; Huang, C. Z. *Biosens. Bioelectron.* **2013**, *43*, 366−371.
(30) Goggins, S.; Naz, C.; Marsh, B. J.; Frost, C. G. *Chem. Commun.* **2015**, *51*, 561−564.
(31) Zheng, Z.; Sun, H.; Hu, C.; Li, G.; Liu, X.; Chen, P.; Cui, Y.; Liu, J.; Wang, J.; Liang, G. *Anal. Chem.* **2016**, *88*, 3363−3368.
(32) Qian, Z.; Chai, L.; Tang, C.; Huang, Y.; Chen, J.; Feng, H. *Anal. Chem.* **2015**, *87*, 2966−2973.
(33) Halawa, M. I.; Gao, W.; Saqib, M.; Kitte, S. A.; Wu, F.; Xu, G. *Biosens. Bioelectron.* **2017**, *95*, 8−14.
(34) Sharma, A. K.; Pandey, S.; Khan, M. S.; Wu, H.-F. *Sensor. Actuat. B-Chem.* **2018**, *259*, 83−89.
(35) Li, J.; Si, L.; Bao, J.; Wang, Z.; Dai, Z. *Anal. Chem.* **2017**, *89*, 3681−3686.
(36) Chen, L.; Yang, G.; Wu, P.; Cai, C. *Biosens. Bioelectron.* **2017**, *96*, 294−299.
(37) Li, D.; Jiang, Y.; Chen, S.; Zhao, Q.; Zhang, Y.; Wang, W.; Sun, Y.; Ma, P.; Song, D.; Wang, X. *Sensor. Actuat. B-Chem.* **2020**, *307*, 127589.
(38) Ma, F.; Liu, M.; Zhang, C.-y. *Chem. Commun.* **2019**, *55*, 8963−8966.
(39) Zhang, L.; Zhao, J.; Duan, M.; Zhang, H.; Jiang, J.; Yu, R. *Anal. Chem.* **2013**, *85*, 3797−3801.
(40) Tan, Y.; Zhang, L.; Man, K. H.; Peltier, R.; Chen, G.; Zhang, H.; Zhou, L.; Wang, F.; Ho, D.; Yao, S. Q.; Hu, Y.; Sun, H. *ACS Appl. Mater. Interfaces* **2017**, *9*, 6796−6803.
(41) Song, Z.; Kwok, R. T.; Zhao, E.; He, Z.; Hong, Y.; Lam, J. W.; Liu, B.; Tang, B. Z. *ACS Appl. Mater. Interfaces* **2014**, *6*, 17245−17254.
(42) Zhang, H.; Xiao, P.; Wong, Y. T.; Shen, W.; Chhabra, M.; Peltier, R.; Jiang, Y.; He, Y.; He, J.; Tan, Y.; Xie, Y.; Ho, D.; Lam, Y.-W.; Sun, J.; Sun, H. *Biomaterials* **2017**, *140*, 220−229.
(43) Zheng, F.; Guo, S.; Zeng, F.; Li, J.; Wu, S. *Anal. Chem.* **2014**, *86*, 9873−9879.
(44) Song, Z.; Kwok, R. T. K.; Zhao, E.; He, Z.; Hong, Y.; Lam, J. W. Y.; Liu, B.; Tang, B. Z. *ACS Appl. Mater. Interfaces* **2014**, *6*, 17245−17254.
(45) Babson, A. L.; Greeley, S. J.; Coleman, C. M.; Phillips, G. E. *Clin. Chem.* **1966**, *12*, 482−490.
(46) Wilson, M. S.; Rauh, R. D. *Biosens. Bioelectron.* **2004**, *20*, 276−283.
(47) Choi, Y.; Ho, N.-H.; Tung, C.-H. *Angew. Chem., Int. Ed.* **2007**, *46*, 707−709.
(48) Freeman, R.; Finder, T.; Gill, R.; Willner, I. *Nano Lett.* **2010**, *10*, 2192−2196.
(49) Li, G.; Fu, H.; Chen, X.; Gong, P.; Chen, G.; Xia, L.; Wang, H.; You, J.; Wu, Y. *Anal. Chem.* **2016**, *88*, 2720−2726.
(50) Deng, J.; Yu, P.; Wang, Y.; Mao, L. *Anal. Chem.* **2015**, *87*, 3080−3086.
(51) Wang, L.-j.; Wang, Z.-y.; Zhang, C.-y. *Analyst* **2018**, *143*, 4606−4613.
(52) Wang, X.; Zhou, S.; Chu, C.; Yang, M.; Huo, D.; Hou, C. *Biosens. Bioelectron.* **2021**, *185*, 113281.
(53) Ma, F.; Liu, W.-j.; Liang, L.; Tang, B.; Zhang, C.-Y. *Chem. Commun.* **2018**, *54*, 2413−2416.
(54) Ye, W.; Li, L.; Feng, Z.; Tu, B.; Hu, Z.; Xiao, X.; Wu, T. *J. Pharm. Anal.* **2021**, na.
(55) Perkins, T. T.; Dalal, R. V.; Mitsis, P. G.; Block, S. M. *Science* **2003**, *301*, 1914−1918.
(56) Ma, F.; Zhang, Q.; Zhang, C.-y. *Nano Lett.* **2019**, *19*, 6370−6376.
(57) Wang, X.; Lim, H. J.; Son, A. *Environ. Anal. Health. Toxicol.* **2014**, *29*, No. e2014007.
(58) Ma, F.; Wei, S.-h.; Leng, J.; Tang, B.; Zhang, C.-y. *Chem. Commun.* **2018**, *54*, 2483−2486.
(59) Barkai, E.; Jung, Y.; Silbey, R. *Annu. Rev. Phys. Chem.* **2004**, *55*, 457−507.
(60) Ma, F.; Li, Y.; Tang, B.; Zhang, C.-y. *Acc. Chem. Res.* **2016**, *49*, 1722−1730.
(61) Narisawa, S.; Harmey, D.; Yadav, M. C.; O'Neill, W. C.; Hoylaerts, M. F.; Millán, J. L. *J. Bone Miner. Res.* **2007**, *22*, 1700−1710.
(62) Liu, G.; Zhao, J.; Yan, M.; Zhu, S.; Dou, W.; Sun, J.; Yang, X. *Sci. China Chem.* **2020**, *63*, 554−560.
(63) Ou-Yang, J.; Li, C.-Y.; Li, Y.-F.; Yang, B.; Li, S.-J. *Sensor. Actuat. B-Chem.* **2018**, *255*, 3355−3363.
(64) Bessey, O. A.; Lowry, O. H.; Brock, M. J. *J. Biol. Chem.* **1946**, *164*, 321−329.

https://doi.org/10.1021/acs.analchem.2c00603
Anal. Chem. 2022, 94, 6004−6010